Controlling the active surfaces of the Velvet Fingers: sticky to slippy fingers.

Vinicio Tincani[†], Giorgio Grioli[‡], Manuel G. Catalano[†‡],
Manuel Bonilla[†], Manolo Garabini[†], Gualtiero Fantoni[†] and Antonio Bicchi[†‡]

***Abstract*— Industrial grippers are often used for grasping, while in-hand re-orientation and positioning are dealt with by other means. Contact surface engineering has been recently proposed as a possible mean to introduce dexterity in simple grippers, as in the Velvet Fingers smart gripper, a novel concept of end-effector combining simple under-actuated mechanics and high manipulation possibilities, thanks to conveyors which are built in the finger pads. This paper undergoes the modeling and control of the active conveyors of the Velvet Fingers gripper which are rendered able to emulate different levels of friction and to apply tangential thrusts to the contacted objects. Through the paper particular attention is dedicated to the mechanical implementation, sense drive and control electronics of the device. The capabilities of the prototype are showed in some grasping and manipulation experiments.**

I. INTRODUCTION

Both in research and in industry, the main use of hands and gripper is to perform the prehensile action. A minor degree of attention is usually devoted to in-hand re-orientation and positioning, tasks that are typically dealt with by using feeders. When such devices are not available and the workpiece has to be re-oriented and positioned in a particular way for further processing, conventional grippers release usually follow a strategy of object release and re-grasp. Such an operation is performed up to several times, during the transfer from one work/assembly station to the next one. [1] During the last decade several devices have been developed to manipulate objects in hand. Some of them are based on the active control of the finger's surface.

A device between a forklift and a gripper has been presented in [2]: it is formed of two forks with actuated belts. Thanks to the independent motion of the belts the forklift gripper can re-orient the grasped object. Moreover two motors can rotate the forks around their own axes, thus enabling the gripper with additional in hand manipulation capabilities. Similarly the "Rack 'n' Roll" gripper [3] has two independent belts. Its capability to move an object in hand has been demonstrated through the handling of a wheel.

Belts have been used also into more complex structures, as that patented by Robin Read [4]. There a twin jaw gripper uses of two interlinked conveyor belts, maintained in constant tension. The length of the belts within the jaws can be varied to modulate the gripping forces. Moreover, proper belt motions allow the grasped object to be rotated in-hand.

[†] Interdepart. Research Center "E. Piaggio", University of Pisa, Via Diotisalvi, 2, 56100 Pisa, Italy.

[‡] Department of Advanced Robotics, Istituto Italiano di Tecnologia, via Morego, 30, 16163 Genova.

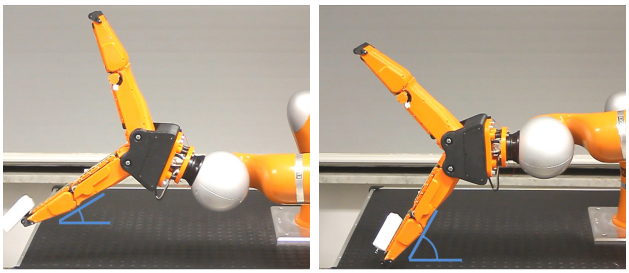

(a) (b)

Fig. 1. Demonstration of different friction levels implemented on the Velvet Fingers dexterous gripper. A test mass of 1kg placed is on one finger (a) and the gripper is slowly inclined. When a lower level of friction is implemented by the controller (b) the mass slides away for a small angle ≈ 19 deg. The highest friction, on the other hand, keeps the mass from sliding until a much higher slope of ≈ 42 deg.

The Traction Gripper [5], presents a very similar principle implemented in a different structure. It consists of a series of active rubber cylinders, arranged on two perpendicular planes, and used as conveying units. Each unit exerts a controlled friction force allowing the grasping of goods of several shapes.

A deeper analysis on in hand manipulation through a gripper with active surfaces can be found in [6].

In [7] the DxGripII was presented, an evolute version of an industrial gripper with dexterous capabilities. The DxGrip-II accomplishes most of the capabilities usually considered in defining dexterity, keeping complexity at a minimum (only 4 actuators are used). It consists of two jaws, whose motions are independently actuated by motors fixed at the base through parallel 4bar linkages. Each jaw has a rotating finger pad actuated by directdrive motors. Finger pads are covered with compliant, high friction material. The distance between the jaws can be varied independently from the distance between the axes of the revolving finger pads, while the jaws always keep their parallel orientation. This dexterous gripper has several modes of operation, as a conventional paralleljaw gripper, with the possibility of translating the grasped object in one direction, as a reorienting device for grasped objects, and as a nongrasping manipulating device.

Similar ideas can also be found in at least other four implementations. For sake of precision we have to mention that, unfortunately, the few information about their design and functioning can be found in web pages, technical brochures or patents rather than in scientific publications.

In hand manipulation is a tricky issue especially in un-

deractuated devices which are usually used for immobilizing the objects with a fixed grasp rather than for dexterity tasks. An intersting attempt to confer dexterity to an underactuated gripper is presented in [8], in which the SDM hand [9] has been modified in order to perform specific planar manipulation tasks. The Velvet Fingers, which prototype was presented in [10], is a further attempt in this direction. It combines the advantages of the underactuation with the dexterity given by the active surfaces, keeping the number of actuator lower than the number of the d.o.f. of the system [11].

This paper presents the control policy that is implemented in the Velvet Fingers gripper to effectively exploit the additional degrees of freedom offered by the presence of the two independent active surfaces. In particular two modalities of control are introduced and shown: a "propulsive mode" in which the active surfaces are used to directly propel the contacted object, and a "variable friction mode" in which the active surfaces are controlled to emulate different levels of friction, allowing the gripper fingers to be like sticky, or slippy, or any halfway behavior.

In sec. II the structure of the Velvet Fingers dexterous gripper is briefly recalled, while sec. III presents in more detail the dynamic model of the active surfaces and the implemented controls. Sec. IV describes the calibration procedures used to tune-up the controller parameters and Sec. V reports of the experimental validation of the capabilities of the gripper, before drawing the final conclusions in sec. VI. Selected highlights of the experiments are also reported in the attached video.

II. SYSTEM DESCRIPTION

Manipulability analysis reported in [11] demonstrates that under-actuated grippers with active surfaces have larger manipulability ellipsoids than a gripper characterized by the same geometry and full actuation. Following this idea, the "Velvet Fingers", a novel underactuated mechanical gripper, has been designed and built ([11], [10]). It has two fingers with two phalanges each, all actuated by one DC motor. The inside of each finger is covered by a conveyor belt active surface that manages contact with the object. Every finger has one motor for the actuation of the conveyors, totaling the number of Degrees of Actuation of the gripper up to three. Fig. 1 shows an overall view of the mechanical implementation of the Velvet Fingers.

One rotary magnetic encoder mounted on the second joint of each finger and one on the motor shaft in the palm, allow to reconstruct the full configuration of the gripper as explained in [10]. One additional magnetic encoder in each finger measures the rotation of the motor roll which angular displacement is related to the linear displacement of the conveyor belt. Two custom electronic boards with PSOC3 micro-controller on board implement the power and logic management. One board takes care of the opening and closure of the gripper whereas the second one controls the conveyor belts as illustrated in Fig. 2. The two controllers communicate with the higher level (a PC with

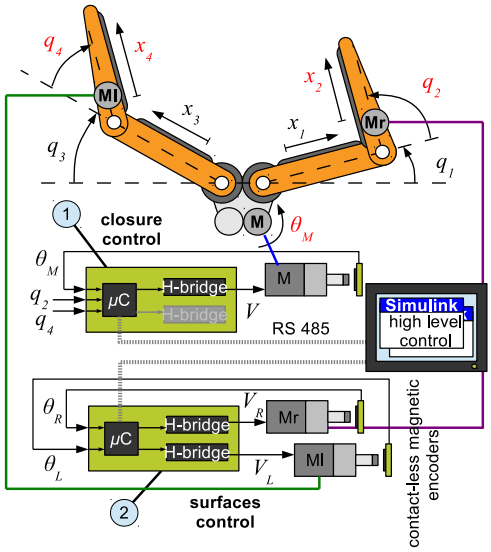

Fig. 2. Control architecture of the Velvet Fingers. The first board controls the motor M for the opening and closure of the gripper and reads the angular position of the second joints $q2$ and $q4$. The second board control the motor M_r and M_l of the active surfaces.

Matlab/Simulink) through a serial RS485 communication link.

An important aspect for the fruitful exploitation of the active contact with the methods described in the next section, is the necessity of high adhesion between the grasped or manipulated object and the active surfaces themselves. In order to maximize this condition the conveyor belts are covered with a flexible high friction material.

III. ACTIVE SURFACES CONTROL

As discussed also in [11], in order to fully empower an underactuated gripper with the benefits offered by active contact surfaces, we propose the implementation of two fundamental functions:

- the **propulsion mode**, in which the active surfaces can apply a tangential push to the contacted object, and
- the **variable friction mode**, in which the apparent friction "felt" by the contacted object is reduced to a defined level.

This section analyzes the dynamic model of the conveyor belt, and defines the two control techniques which allow the implementation of the two described fundamental functions.

A. Conveyors model

In first approximation the dynamic model of the conveyor belt system can be modeled as in Fig. 3, consisting in a three Degrees of Freedoms (DoFs) system, where a mass M (the gripper payload) is in perfect adhesion with the belt which winds around a motor and an idle roller. The longitudinal elasticity of the belt can be modeled with three lumped linear springs, and finally each components is linked to a linear damper in order to account for energy losses.

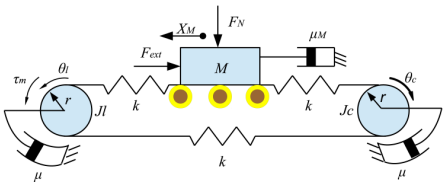

Fig. 3. Dynamical model of the conveyor belts. It is a three DoFs system which Lagrangian coordinates (θ_l, θ_c, x_m) are linked through springs with elasticity constant k. The mass M is subjected to normal (F_N) and tangential (F_{ext}) external forces. Driving roller (radius r and moment of inertia J_l, included rotating elements of the DC motor) is actuated by motor torque τ_m. Driven roller has radius r and moment of inertia J_c. Damper elements are included to account of the energy dissipation.

The dynamic equations of the system follow:

$$\begin{cases} \ddot{\theta}_l = & \frac{1}{J_l}\Big(-\mu\dot{\theta}_l - kr(\theta_l r - x_M) - kr^2(\theta_l - \theta_c) + \\ & + \frac{k_\tau n_m}{R}\left(V - k_c n_m \dot{\theta}_l\right)\Big) \\ \ddot{\theta}_c = & -\frac{1}{J_c}\left(\mu\theta_l + kr(\theta_c r - x_M) + kr^2(\theta_c - \theta_l)\right) \\ \ddot{x}_M = & \frac{1}{M}\left(F_{ext} - \mu_M \dot{x}_M - k(x_M - \theta_l r) - k(x_M - \theta_c r)\right) \end{cases} \tag{1}$$

where the new parameters introduced are the tension applied to the motor V and its electrical resistance R the torque and speed constant k_τ and k_c, and the transmission ratio from the motor to the driving roller n_m respectively.

This dynamical system is already stable (which can be demonstrated thanks to simple passivity considerations), and can be easily controlled thanks to the closure of a simple proportional loop on the motor position. We will see in short as this is, in fact, the fundamental building block for the two control modes of the active surfaces.

B. Propulsion mode control

The force equilibrium on the lumped mass considered on the belts yields that any torque generated by the conveyor motor is then transmitted to the contacted object. Thus, actuating the conveyor belt, when the object is grasped inside the fingers of the gripper, it is possible to perform tasks of in hand manipulation as shown in Fig. 4.

Tangential push control mode is obtained through direct control of the tension V applied to the motor driving the belt, accounting for proper transmission ratio. To apply a desired tangential force F_t on the contacted object, a tension

$$V = F_t \frac{rR}{k_\tau n_m}, \tag{2}$$

is provided to the motor. In applying this control both the electric dynamics of the motor current and the counter electro-motive force (CEMF) on the motor rotor are neglected. This is possible due to the relatively slow dynamics of the manipulation which, on one side, are orders of magnitude slower than the electric dynamics, and on the other imply very small induced CEMF. Given this result, the same simplification was used also for the next modality of control.

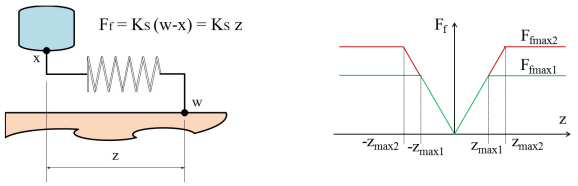

(a) (b)

Fig. 5. Friction model with virtual spring (a). Different values of F_{fmax} obtained by setting different thresholds of z_{max} (b).

C. Variable friction mode control

Variable friction mode is obtained by applying the algorithm proposed in [12]. In emulating friction two important assumptions are made:

1) friction is simulated in terms of its total resulting action, and
2) kinetic friction is assumed equal to the maximum static friction.

While the first assumption is demanded by the physical implementation of the active surfaces, i.e. conveyors, the second assumption allows to simplify the control of both the conveyors and the manipulation, by allowing more stable and predictable controlled sliding.

Given a desired static friction coefficient ν, it yields a desired maximum friction force $F_{fmax} = \nu F_N$ where F_N is the total normal force exerted on the contact. The algorithm proposed in [12] models the friction force as a virtual spring between the object and the plane, with stiffness K_s, lenght at rest null and maximum elongation z_{max}. One side of the spring is attached on the contacted object at point x, the other side is fixed to the surface at point w, its elongation is $z = w - x$ and the emulated friction force is given by $F_f = K_s(w-x)$ (Fig. 5(a)). As long as z is smaller than z_{max}, w is sticked on the surface, while, when z reaches the z_{max} value, the spring becomes rigid, no further elongation is permitted and w is dragged toward the (displaced) object. For a given K_s, the maximum emulated friction force F_{fmax} can be tuned by choosing the value of z_{max} as shown in Fig. 5(b).

This is implemented by the following discrete-time system laws:

$$\begin{cases} w(i+1) = \begin{cases} x(i) - z_{max} & \text{if} \quad x(i) - w(i) > z_{max} \\ w(i) & \text{if} \quad |x(i) - w(i)| < z_{max} \\ x(i) + z_{max} & \text{if} \quad x(i) - w(i) < -z_{max} \end{cases}, \\ \\ F_f(i) = K_s SAT^{z_{max}}_{-z_{max}}(x(i) - w(i)) \end{cases} \tag{3}$$

where i indicates the sampling time, and $SAT^b_a(z)$ is the saturation of z to the interval $[a,b]$. In the algorithm the first block is the updating of the virtual reference $w(i)$ and the real linear displacement x is related to the angular displacement of the motor roll of the belt and thus it can be read by the encoder.

1) Simulations: Theoretically, by changing the saturation threshold of the torque resisting to the sliding of a mass

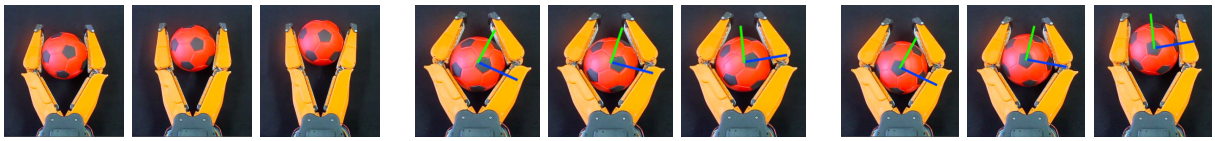

Fig. 4. In hand manipulation of a spherical object. The translation movement is obtained making the motors of the belts counter-rotate with the same angular speed (first three frames). By rotating the motors with the same intensity and direction, the ball is rotated (second three frames). The roto-translation movement is obtained actuating the motors with different in modulus angular speed (last three frames).

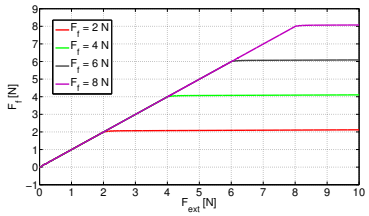

Fig. 6. External pushing force Vs tangential emulated friction force. Simulation of different levels of emulated friction.

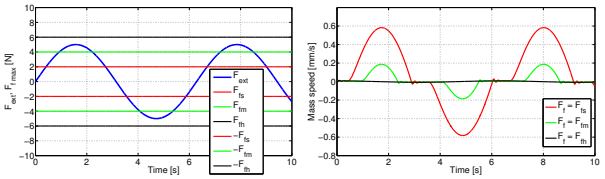

(a) (b)

Fig. 7. Tangential response of the active surface to external force for different levels of friction. Simulation shows the different behaviors of the contacted object when it is externally pushed/pulled with a force $F(t) = 5\sin(t)$, over a ten second time interval, with different levels of emulated friction. Left panel shows the external force and the three thresholds of static friction $f_{fs} = 2N$, $f_{fm} = 4N$ and $f_{fh} = 6N$. Right panel shows the speed of the contacted object in the three different cases.

located above the conveyor belt and subjected to an external force directed along the direction of the movement of the belt, it is possible to emulate the situation in which the mass is standing on different surfaces with different friction coefficient. Fig. 6 and Fig. 7 show the results of two simulations that implement the previous claim in a Matlab/Simulink environment. The first plot shows the friction force as function of the external force for different emulated friction coefficient. The second one shows the behaviour of the speed of the mass under a sinusoidal external force and it allows to test the correctness of the model in presence of stops and motion inversions as well.

The behavior observed in simulation if coherent with the theoretical friction model, ia accordance to [12].

IV. SYSTEM CALIBRATION

In practice, the emulated friction coefficient depends on the real physical system that implements the variable friction. Indeed, it is limited by an upper bound given by the incipient sliding between the belt and the object, and a lower bound given by the parasitic internal friction of the mechanical transmission system. In order to widen the most this range, conveyor belts are painted with high friction gum, and all the rotating components are sustained by ball bearings. Moreover

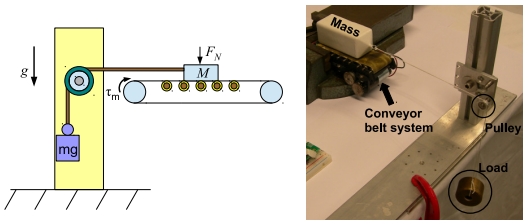

Fig. 8. Experimental set up used for the calibration of the control system of the variable friction.

the motor has high-efficiency gears with a low reduction ratio, to allow a retrograde motion with the lowest resistance possible.

Nevertheless, the presence of all the parasitic frictions in the system requires for a preliminary calibration phase. This calibration was carried out with the experimental set up shown in Fig. 8.

A limitation of the system, which arose during the calibration tests, was found to be the relatively high parasitic friction introduced by the serial transmission of the conveyor movement among both phalanges of the same finger. This hindered severely the performance of the system. To remedy this situation, a careful optimization of the transmission system would have been required. Given the impossibility to change the design of the transmission in short time, a small modification was introduced in the system: the transmission between the two phalanges of the same finger was eliminated. This strongly reduced the amount parasitic friction and did not tamper much the overall functionality of the Velvet Fingers' active surfaces, given that the surfaces of distal phalanges, the most used for the majority of the tasks, were the one still active after the introduced modification. By virtue of this, all the results reported in this paper concern a simplified version of the Velvet Fingers dexterous gripper, where only the two distal phalanges have active surfaces.

A. Calibration setup of one phalanx

The distal phalanx has been fixed horizontally. Two different masses have been placed on the belt to simulate two different normal forces F_N of $10.7N$ and $21.4N$. Other masses m_g have been linked to the ones on the belt through a wire winding on a pulley to simulate different external tangential forces $F_{ext} = m_g g$. The calibration phase allows to establish the effective correspondence between the saturation level of the tension V applied to the motor and the wanted fictitious friction coefficient, for each normal load. The effective saturation threshold is determined by the level of the tension in

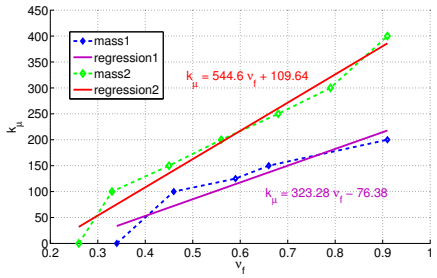

Fig. 9. Calibration curves and regression lines for each normal load.

which the masses start to move. Fig. 9 shows the calibration curves and their regression lines for the two normal load, in which k_μ is a proportionality constant between z_{max} and the tension V. The variation of the emulated friction coefficient varies from 0.34 up 0.91 for the smallest load and from 0.26 up to 0.91 for the largest one.

B. Calibration results

The results of the calibration show a wide range of variation of the apparent friction coefficient with a very high upper limit and a lower limit decreasing with the enhancement of the normal load applied. The internal friction of the system prevents to obtain low friction coefficient with low normal loads. The obtained range is however satisfying for the load applied by the Velvet Fingers to the object (that can exert a compression force of $18N$ when the piece is grasped on the tips of the fingers) and the effect of the variable friction are described in the next section. To further decrease the internal friction and thus to lower the lower limit, other expedients (not implemented in the Velvet Fingers) can be adopted, such as using convex rolls to avoid the axial sliding of the belts and therefore the contact with the frame and simplifying the rolls disposition as much as possible (for example arranging the rolls along a straight line).

V. EXPERIMENTAL VALIDATION

In this section we present several applications examples where a combination of the gripper closure movement and the two control modes of the active surfaces allow the successful grasp and manipulation of different objects characterized by various shapes. To perform these experiments, the Velvet Fingers is mounted on a KUKA LWR IV robot manipulator using a compliant wrist. This expedient is motivated by the desire to avoid damages to the system when dealing with uncertainty in position of the gripper and the object to be grasped.

Experiments are divided in two groups. The first group is realized using mostly propulsion mode control, the second group, on the other hand, explores the possibilities offered by variable friction mode control.

A. Propulsion mode possibilities

This experiment was performed to simulate a scenario where the task is to grasp a very wide box. The box is so wide that the gripper cannot perform an enveloping grasp around

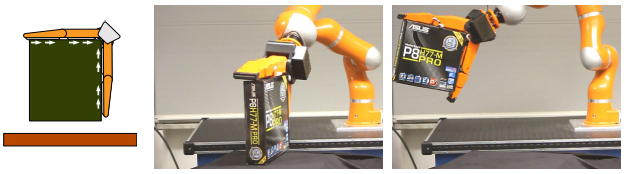

Fig. 10. Increased grasping ability trough direct application of propulsive action. The active surfaces are used to propel the grasped box in the inward direction, effectively sucking it, and allowing a firm grip.

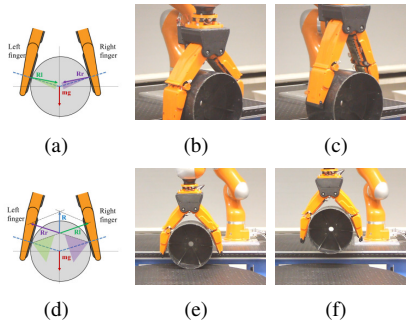

Fig. 11. Grasping a cylinder with low and high friction. The left three frames shows the unsuccessful attempt to grasp a big cylinder above its diameter due to the low friction. On the other hand, in the three rightmost frames, high friction is set on the active surfaces. The wide friction cones (d) allow to balance the weight of the cylinder and then to lift it (f).

it. This is shown in Fig. 10, where the black cardboard box is grasped on the largest dimensions. This problem can be solved by generating tangential forces on the faces of the box to let it remain in contact during lifting. In the case of the Velvet Fingers this task is performed using the tangential thrust generated when a position control is implemented on the conveyor belts, which effectively generate a suction effect on the object, allowing it to be grasped.

B. Variable friction mode possibilities

Grasping a cylinder can be a challenging task when it is not possible to contact the object under its diameter. To do it, it is necessary that the normal forces exerted by the gripper have a vertical component big enough to balance the weight of the object, otherwise the piece tends to fall down. To avoid the last situation we can squeeze the cylinder and at the same time impose high friction on the active surfaces (see Fig. 11).

Another example where application of high friction is demanded is when an external torque, normal to the closure plane of the gripper, is imposed on the grasped object. Under this condition it is necessary to compensate this torque to maintain the object unmovable. See Fig. 12 where a task of bottle opening is presented as an example.

C. Applications Using Low Friction

The aim of this experiment is to grasp a box under a cluttered environment, meaning that the box is located between objects which reduce the possibilities to pose the Velvet

(a) (b) (c) (d) (e) (f)

Fig. 13. Different grasp equilibria triggered by different levels of friction. The two sequences, left and right, show the evolution of two grasps starting from same initial conditions but yielding different final configurations thanks to different levels of controlled friction. While on the left sequence high friction ensures stability for the initial grasping configuration, on the right a lower friction level let the grasped object slide in a different configuration.

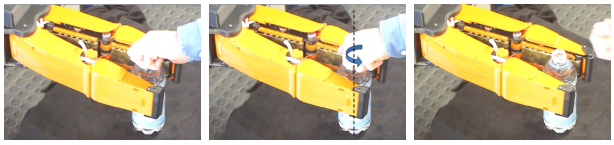

(a) (b) (c)

Fig. 12. High friction can be used to balance the torque applied to screw-open the cap of a grasped bottle.

(a) (b) (c)

Fig. 14. The Velvet Fingers can exploit low friction in case of cluttered environments. The figure shows the grasp of a box from on high with reduced possibility of opening (a). With low friction the box get into the fingers when the gripper push down the object (b). Once grasped, imposing high friction, the box is lifted.

Fingers and easily perform a stable grasp (see Fig. 14). Due this scenario, and taking advantages of the active surfaces, we set the active surfaces to low friction and then pushed the Velvet Fingers down the object to force it to get into the fingers and grasp it (see Fig. 14(b)). Once grasped, the object is lifted up using high friction.

D. Combining High and Low friction

This experiment shows the skills of the Velvet Fingers to grasp a cube by its edges. Taking advantages of the active surfaces on velvet fingers and inducing high friction force in one belt and low in the other, the cube is able to rotate and get a bigger contact area with one of the fingers as explained in Fig. 13. Doing this, it is not necessary to plan the pose of the Velvet fingers to perform a stable grasp, instead, it can be achieved using active surfaces to drive the object to change its orientation. This strategy makes the difference between a common gripper and the Velvet Fingers is that while the first performs a rigid grasp, the second allows to do this and also to perform passive in-hand manipulation.

VI. CONCLUSIONS

The present work described the design and application of the control of the active surfaces of the Velvet Fingers smart gripper, a novel kind of end-effector recently presented in [11] and [10].

Two modalities of control were introduced and shown: "propulsive mode" and "variable friction mode". Both modalities offer advantages in terms of achievable grasps and manipulability aids. Experiments describing both the calibration of the controllers parameters and the augmented gripper dexterity were described and shown, also in the attached video footage.

ACKNOWLEDGEMENTS

The authors wish to gratefully acknowledge Fabio Bonomo, Felipe Belo, Edoardo Farnioli, Alessandro Serio, Alberto Brando, Andrea di Basco, and Fabrizio Vivaldi for their valuable help. The research leading to these results has received funding from the European Union Seventh Framework Programme [FP7/2007-2013] under grant agreements n ICT-270350 (project ROBLOG) and ERC Advanced Grant 291166 (Soft-Hands).

REFERENCES

[1] P. Datseris and W. Palm, "Principles on the development of mechanical hands which can manipulate objects by means of active control," in *Journal of Mechanisms, Transmissions, and Automation in Design*, vol. 107(2). ASME, 1985, pp. 148–156.

[2] "Roboter mit aufwaelzgreifer wird zum multitalent fuer die lagerlogistik," http://www.ipa.fraunhofer.de/fileadmin/-www.ipa.fhg.de/Presse/Pressemitteilung/PR_Automatica.pdf, Fraunhofer-Institut fuer Materialfluss und Logistik IML, in German.

[3] B. Mello, "First "rack n' roll" manupilator design," http://www.slideshare.net/guestf64799/rack-n-roll-manipulator-idea.

[4] G. Read, R., "Robotic hand effector," US Patent GB 2 459 723, 2009.

[5] "Traction gripper systeme – reibschluessiges greifen von stueckgut," http://www.iml.fraunhofer.de/content/dam/iml/de/documents/-OE%20140/Traction%20Gripper%20Systeme.pdf, Fraunhofer-Institut fuer Materialfluss und Logistik IML, in German.

[6] A. Bicchi, "Hands for dexterous manipulation and robust grasping: A difficult road toward simplicity," *Robotics and Automation, IEEE Transactions on*, vol. 16, no. 6, pp. 652–662, 2000.

[7] A. Bicchi, A. Marigo, and D. Prattichizzo, "Dexterity through rolling: Manipulation of unknown objects," in *Robotics and Automation, 1999. Proceedings. 1999 IEEE International Conference on*, vol. 2. IEEE, 1999, pp. 1583–1588.

[8] L. U. Odhner and A. M. Dollar, "Dexterous manipulation with underactuated elastic hands," in *Robotics and Automation (ICRA), 2011 IEEE International Conference on*. IEEE, 2011, pp. 5254–5260.

[9] A. M. Dollar and R. D. Howe, "The highly adaptive sdm hand: design and performance evaluation," *The international journal of robotics research*, 2010.

[10] V. Tincani, G. Grioli, M. G. Catalano, M. Garabini, S. Grechi, G. Fantoni, and A. Bicchi, "Implementation and control of the velvet fingers: a dexterous gripper with active surfaces," in *IEEE International Conference on Robotics and Automation (ICRA2013)*, In Press.

[11] V. Tincani, M. G. Catalano, E. Farnioli, M. Garabini, G. Grioli, G. Fantoni, and A. Bicchi, "Velvet fingers: A smart gripper with controlled contact surfaces," in *International Conference of Intelligent Robots and Systems - IROS 2012*, Vilamoura, Algarve, Portugal, October 7 - 12 2012.

[12] V. Hayward and B. Armstrong, "A new computational model of friction applied to haptic rendering," *Experimental Robotics VI*, pp. 403–412, 2000.